SUPPLEMENTAL MATERIALS

PCSK9 deficiency results in a specific shedding of excess LDLR in female mice only: role of hepatic cholesterol

Anna Roubtsova (Msc)[1], Damien Garçon (PhD)[1], Sandrine Lacoste (PhD)[1,6], Ann Chamberland (BSc)[1], Jadwiga Marcinkiewicz (MSc)[1], Raphaël Métivier (PhD)[2], Thibaud Sotin (MSc)[1,4], Carl P. Blobel (MD, PhD)[3], Martine Paquette (Msc)[1], Sophie Bernard (MD, PhD)[1], Bertrand Cariou (MD, PhD)[4], Cédric Le May (PhD)[4], Marlys L. Koschinsky (PhD)[5], Nabil G. Seidah (PhD)[1] and Annik Prat (PhD)[1]*

[1]Institut de Recherches Cliniques de Montréal (IRCM), affiliated to the Université de Montréal, Montreal, QC, Canada
[2]Equipe SP@RTE, UMR 6290 CNRS, Université de Rennes 1, Rennes, France
[3]Arthritis and Tissue Degeneration Program, Hospital for Specialized Surgery at Weill Cornell Medicine, New York, USA
[4]Université de Nantes, CNRS, INSERM, l'Institut du thorax, F-44000 Nantes, France
[5]Robarts Research Institute, Schulich School of Medicine & Dentistry, Western University, London, ON, Canada
[6]S.L. present address: Centre de recherche de l'hôpital Maisonneuve Rosemont, Montreal, QC, Canada

SUPPLEMENTAL METHODS

Mice, diets and blood collection (more detailed information)

Mice were housed in enriched cages on corn cob bedding, and usually euthanized after 3 hours of fasting from 7 to 10 am. The lovastatin diet was constituted as follows: one hundred lovastatin tablets (200 mg; each containing 20 mg of lovastatin; DIN 02220172, Aapharma inc, Toronto, Canada, L4K4N7) and 1 kg of our regular laboratory diet were separaterly grinded and mixed. Food balls were then reconstituted by adding 500 mL of sterile water. Blood was collected in heparin-coated Microtainer tubes (Becton Dickinson, Franklin Lakes, NJ) or heparinized micro-hematocrit capillaries (Fisher Scientific, Pittsburg, PA), centrifuged for 5 min at 3800g at 4°C, and kept at -80°C until assayed.

LDLR immunohistochemistry (more detailed information)

Images were acquired using the LSM700 confocal microscope under ZEN2011 software (Zeiss, Jena, Germany). Original Zen format images were opened with Imaris software (Oxford Instruments, Zürich, Switzerland), and data values transferred to custom Matlab (MathWorks Inc, Natick, MA) using the Imaris XTension module (Oxford Instruments). For every image, pixel values comprised between 21 and 255 (maximum value in non-saturated conditions) were summed, the negative control value was subtracted, and the final sums were analyzed. Representative pictures are shown in figures. Although intracellular compartments are exposed in 8 mm-thick cryosections, a quasi-exclusive labeling of cell surface LDLR was observed. In agreement, the 4-fold increase observed in KO male liver sections by immunohistochemistry was confirmed by liver subcellular fractionation, and LDLR Western blotting of plasma membrane-enriched fractions [1].

Western blotting

Total proteins were extracted from liver pieces and analyzed by PAGE, as described previously.

Quantitative RT-PCR

As described previously [1], total RNA was extracted from frozen liver pieces with TRIzol reagent (Invitrogen, Carlsbad, CA), and reverse transcribed into cDNA using a SuperScript II cDNA reverse transcriptase and RNase OUT inhibitor (Invitrogen). QPCR was performed using PowerUp SYBR Green Master mix (ABI, Fisher Scientific) on Applied Biosystems VIIA 7 Real-Time PCR system. All gene expressions (see Table of primers) were normalized to that of hypoxanthine-guanine phosphoribosyltransferase (*Hprt*) or TATA-binding protein (*Tbp*).

RNA-SEQ (more detailed information)

Read quality was assessed using FastQC v0.11.5 [2]. Read alignment was performed using STAR v2.5 [3] on the mm10 mouse reference genome. Differential expression analysis was performed with DESeq2 v1.22.2 [4] from the raw alignment counts computed with featureCounts 1.4.6 [5] based on the Ensembl annotation release 93. Group effect (PCSK9 WT or KO) was added as a fixed-effect in the model to test for the effect of estradiol E2 (or placebo), while controlling for the known variation linked to the presence or absence of the PCSK9 gene. Differentially expressed genes were then defined as genes with an adjusted p-value < 0.05 and Fold change (counts) >1.5. RNA-Seq data are available from GEO (https://www.ncbi.nlm.nih.gov/geo/query/acc.cgi?acc=GSE205008).

References

[1] A. Roubtsova, A. Chamberland, J. Marcinkiewicz, R. Essalmani, A. Fazel, J.J. Bergeron, N.G. Seidah, A. Prat, PCSK9 deficiency unmasks a sex/tissue-specific subcellular distribution of the LDL and VLDL receptors in mice, Journal of Lipid Research, 56 (2015) 2133-2142.
[2] A.D. Smith, FastQC: A quality control tool for high throughput sequence data in, http://www.bioinformatics_babraham_ac_uk/projects/fastqc/, 2010.
[3] A. Dobin, C.A. Davis, F. Schlesinger, J. Drenkow, C. Zaleski, S. Jha, P. Batut, M. Chaisson, T.R. Gingeras, STAR: ultrafast universal RNA-seq aligner, Bioinformatics, 29 (2013) 15-21.
[4] M.I. Love, W. Huber, S. Anders, Moderated estimation of fold change and dispersion for RNA-seq data with DESeq2, Genome Biol, 15 (2014) 550.
[5] Y. Liao, G.K. Smyth, W. Shi, featureCounts: an efficient general purpose program for assigning sequence reads to genomic features, Bioinformatics, 30 (2014) 923-930.

Primers

Gene	Forward	Reverse
Hprt	5′-CCGAGGATTTGGAAAAAGTGTT	5′-CCTTCATGACATCTCGAGCAAGT
Tbp	5′-GCTGAATATAATCCCAAGCGATTT	5′-GCAGTTGTCCGTGGCTCTCT
Ldlr	5′-GGAGATGCACTTGCCATCCT	5′-AGGCTGTCCCCCCAAGAC
Hmgcr	5′-GTACGGAGAAAGCACTGCTGAA	5′-TGACTGCCAGAATCTGCATGTC
Pcsk9	5′-CACCTTCCGCCGTTGCT	5′-CCTCTGGGTCTCCTCCATCA
Srepb2	5′-GTTCTGGAGACCATGGAG	5′-AAACAAATCAGGGAACTCTC
Esr1	5′-GCTGCAAGGCTTTCTTTAAGAGA	5′-TTGGTTTGTAGCTGGACACATGT
Esr2	5′-CATCAGTAACAAGGGCATGGAA	5′-CCGGGACCACATTTTTGC
Gper1	5′-CTCCCCTTAAGCTGCTGGAA	5′-GGGCACCCAGAGTGTGTGA
Aurkb	5′-ATGGCTCAGAAGGAGAACGC	5′-CCGTAGGACTCTCTGGGACA
Bub1b	5′-CCAAGGAGAGACGCGCTATT	5′-GGCAAGGGAAACGCCAATTC
Ccnb1	5′-TGTGTGAACCAGAGGTGGAAC	5′-ATGTTTCCATCGGGCTTGGAG
Cdc20	5′-GAGTGCTGTGGATGTGCATT	5′-GCAAAGCCGTGACCTGAGA
Cenpe	5′-GAAAATTCTCTCATGAAGTTCGGA	5′-CTCCACTCTACCTCAGCCAA
Ckap2l	5′-GAACGGGGCAACACCAGTA	5′-AGCTGAGGTGTCAGAGGTTAC
Dlgap5	5′-GAATGCCACCTTCTTGAACCA	5′-GAGAACTGTCTGCTGCGATCT
Foxm1	5′-ATCACGGAGACGTTGGGAC	5′-CCACTGGATATTGGTTAAGCTGT
Hmmr	5′-AACCAGAGCCAACGAGCTAC	5′-TCCTGTTTGACCATCATACTCC
Kif20a	5′-TCTCTGCCTCTCTGGAGGAC	5′-AAGGAGTCTTTGGGTGCCTG
Kifc1	5′-GACGCGGGTCTCATCGTC	5′-TCACTTCCAACAAAGGTGGCCT
Knstrn	5′-AACCCACCACAGATCACACG	5′-ACTGGACACTCTCCTCTTCTT
Plk1	5′-TCACCATCCCACCAAGGTTT	5′-CTCATTTGTCTCCCGGACCA
Prc1	5′-AGAAGTCTGGCAAAGTACGCA	5′-TGACAACTGACTTGCTGCCA
Racgap1	5′-TACTACAATGGTGAATTTGTGGAC	5′-CGAAGTCCTTCACAACCTGGA
Spag5	5′-CAGGCCCTAGAGAAGACACAC	5′-TCATTGGACAGAGGGTGTTCC
Top2a	5′-CCTCGGGGCAAAAGAGTCAT	5′-CTATTCGTTGCCGGAGGCTT
Ttk	5′-CACCCCGAAGGCTGACAAAG	5′-AGCTGGCTGTAAGGTGTTGA
Adam10	5′-CCTACGAATGAAGAGGGACAC	5′-ACTAAAGCTTCCTTCTTCACCAT
Adam17	5′-GCAGAATATAACGTAGAGCCACT	5′-CTCTCTGTCTATGAGCCCTTTTG

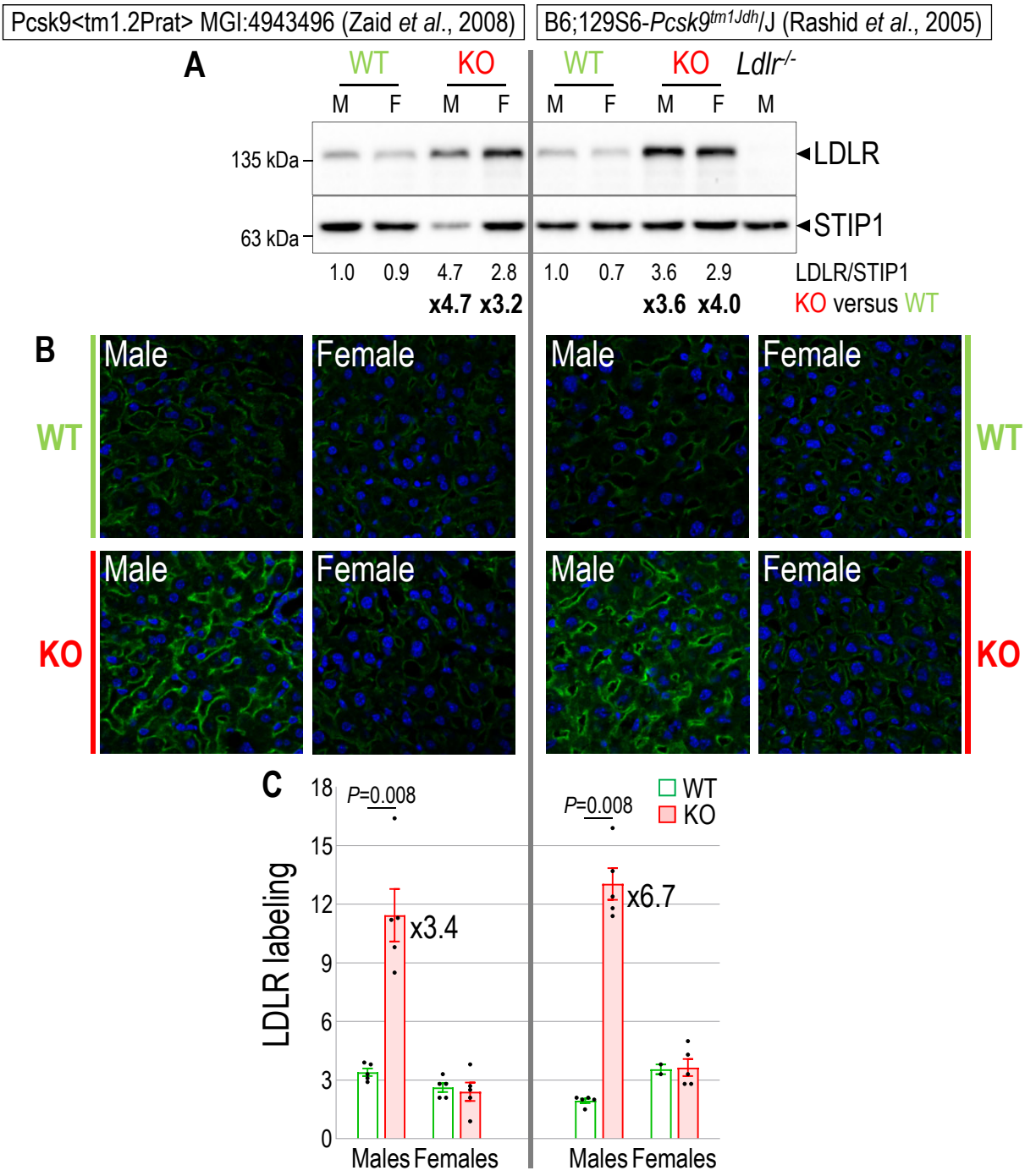

Figure S1. Hepatocyte surface levels of the LDLR are sex-sensitive in PCSK9 KO mice.
In the mouse model used in this study, *loxP* recombination led to the excision of *Pcsk9* proximal promoter and entire exon 1 (left panels). In the second mouse model (right panels), a neomycin-resistance cassette replaces the region comprising exons 1 to 3 of *Pcsk9*. The two mouse strains underwent ≥12 backcrosses with C57BL/6J mice. **A**, The total liver protein levels of the LDLR were assessed by Western blotting in WT and PCSK9 KO littermates and normalized to those of STIP1 (~65 kDa; 1:1000, Abcam. Toronto, ON), which is not significantly affected by the absence of PCSK9 (Roubtsova *et al.*, 2015). **B**, Representative images from LDLR immunohistochemistry on cryosections from WT or KO male and female livers. **C**, LDLR labeling quantification. n=5 mice. Mean±SEM. *P* values were determined using Mann-Whitney *U* test (non parametric data).

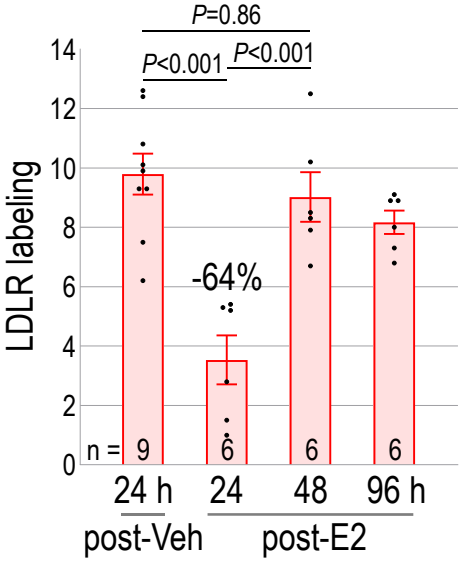

Figure S2. E2-mediated reduction of LDLR immunohistochemical labeling is transitory.
Ovariectomized PCSK9 KO females received an intraperitoneal injection of vehicle (Veh) or 1 ug of cyclodextrin-encapsulated E2 (50 μg/kg) at 9:00 am. Mice were euthanized 24, 48 or 96h later. n=6-9 mice. LDLR immunohistochemical labeling of liver cryosections was quantified. Mean±SEM. *P* were determined by using 1-way ANOVA followed by Tukey's multiple comparisons test.

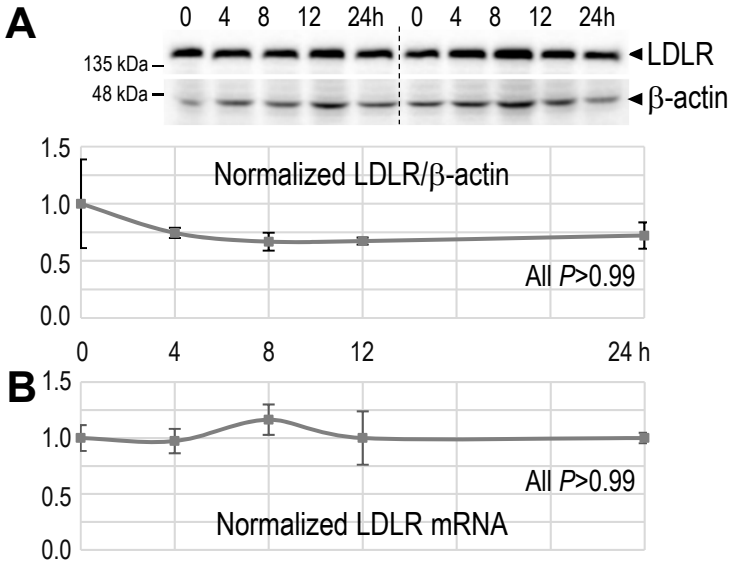

Figure S3. Total LDLR liver expression is not regulated by E2 in PCSK9 KO males.
KO male mice did not receive (t = 0) or received an IP injection of 1 μg of E2. **A,** Representative blot of the analysis of liver LDLR protein with goat anti-LDR (R&D systems, Minneapolis, MA) and rabbit anti-mouse β-actin (Sigma-Aldrich, St. Louis, MO). **B**, mRNA levels were estimated by QPCR. n=3-4 mice. Mean±SEM normalized to t=0. Absence of significant changes was confirmed using Kruskal-Wallis test followed by Dunn's multiple comparisons test (non parametric data).

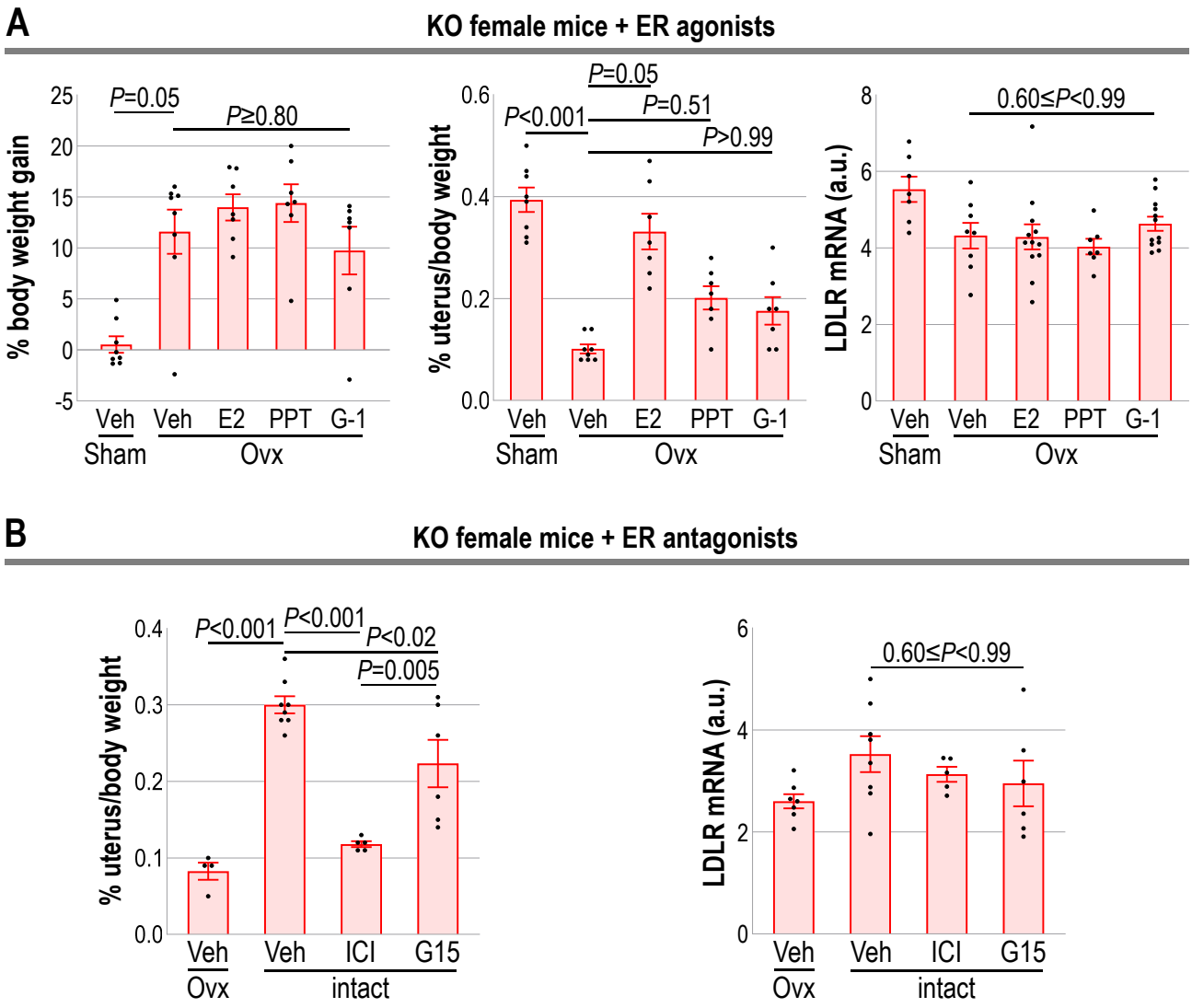

Figure S4. In PCSK9 KO mice, E2 reduces LDLR density at the hepatocyte cell surface via ERα.
Mice analyzed in Figure 2 were further characterized. **A**, PCSK9-deficient female mice were sham-operated or ovariectomized (Ovx) and injected with vehicle, E2 or the ERα and Gper1 agonists, PPT and G-1, respectively. **B**, Ovariectomized or intact PCSK9-deficient female mice were injected with vehicle, ERα and ERβ inhibitor ICI 182,780 or Gper1 inhibitor G15. Ovx-related body weight gain (A only) and uterus weight are expressed as percents of the body weight. As expected, Ovx mice had a higher gain weight in 2 weeks than sham-operated mice. E2, PPT and G-1 treatment allowed an 80%, 34% and 25% recovery of the uterus weight, respectively. The partial, but highly significant (P = 0.001) effect of PPT is in agreement with the single low dose injected in this study (Frasor *et al.*; ref. 51), while G-1-mediated recovery (P = 0.02) may be due to epithelium proliferation (Dennis *et al.*; ref. 52). n=7-8 mice. Mean±SEM. P values were determined using Kruskal-Wallis test followed by Dunn's multiple comparisons test (non parametric data; **A**, two left panels) or 1-way ANOVA followed by Tukey's multiple comparisons test (all other panels).

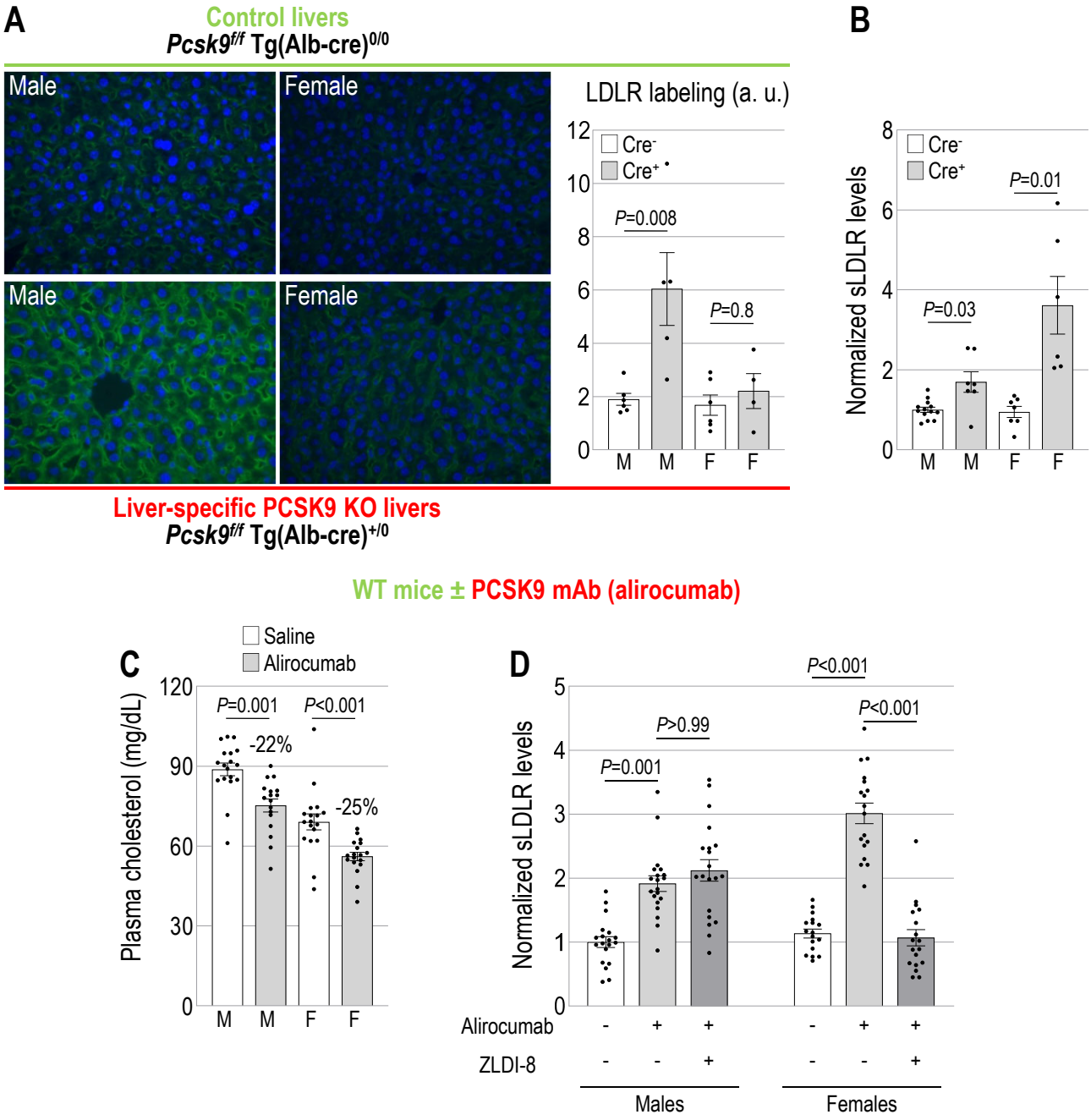

Figure S5. The loss of liver PCSK9 or neutralization of its circulating form leads to the same sex-specific LDLR pattern than the one observed in whole body PCSK9 KO mice. A, LDLR immunohistochemistry was performed on liver sections from control and liver-specific PCSK9 KO littermates on the C57BL/6J genetic background.[6] Quantitation of the LDLR immunolabeling generated the same pattern than in Figure 1A. n=5 mice. **B**, Plasma sLDLR levels were assessed in the same mice, and found similar to those obtained in Figure 3A. n=6-13 mice. **C**, Plasma cholesterol and **D**, sLDLR levels were measured in WT male and female mice that received one subcutaneous injection of saline or alirocumab (50 mg/kg; Praluent, Sanofi Canada Inc.). sLDLR levels were also measured 8 hours post-ZLDI-8 injection (10 mg/kg). n=17-20 mice. Mean±SEM. *P* values were determined using Mann-Withney *U* test (non parametric data; **A**), Student's t-test with Welch's correction (**B**), and Kruskal-Wallis test followed by Dunn's multiple comparisons test (non parametric data; **C** and **D**).

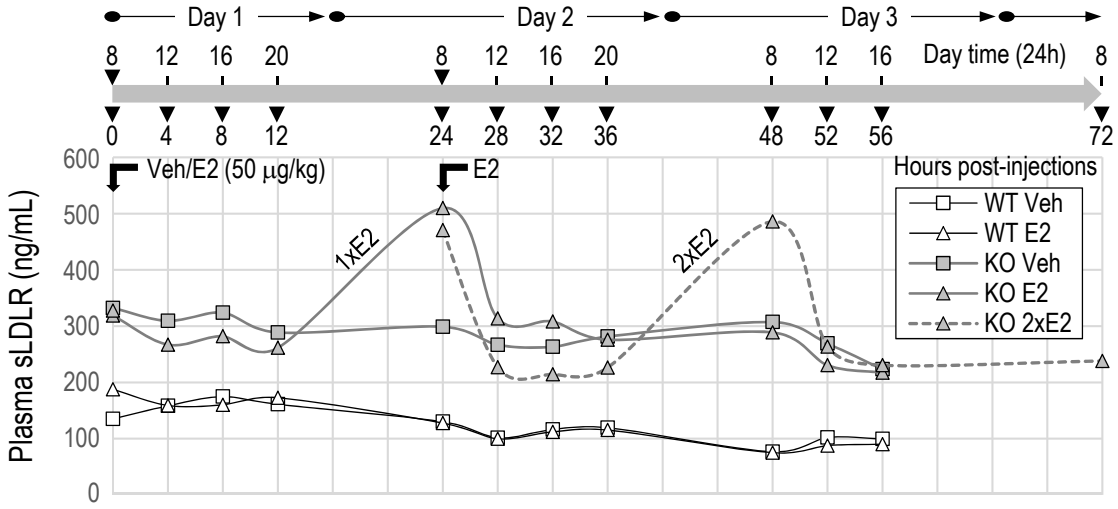

Figure S6. In the absence of PCSK9, E2 increases LDLR shedding in male mice.
WT or KO male mice received vehicle (Veh) or E2 by intraperitoneal injection (50 µg/kg). At t = 24 h, half of the E2-treated KO male mice received a second dose of E2 (50 µg/kg) that generated a similar peak of plasma sLDLR, indicating that surface LDLR density was rapidly replenished after the first shedding peak. n=4-5 mice.

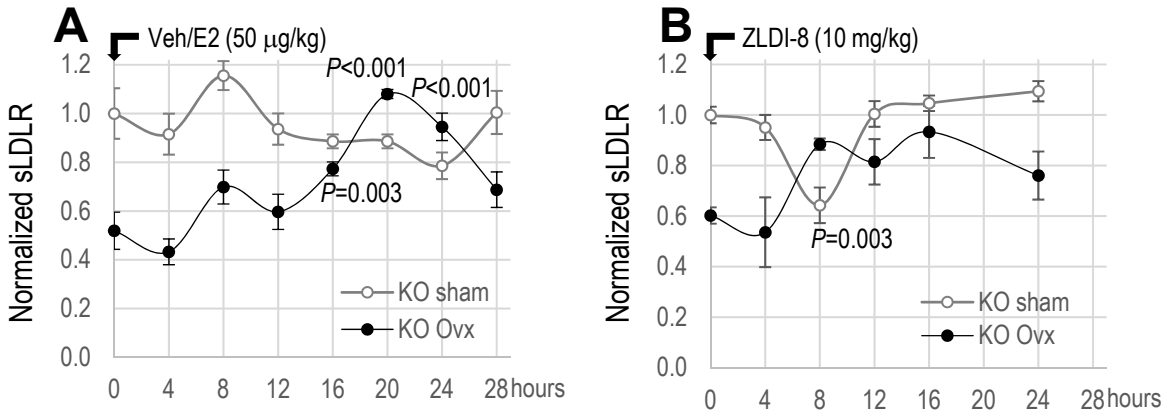

Figure S7. E2 increases and ZLDI-8 inhibits LDLR shedding in PCSK9 KO ovariectomized or sham-operated mice, respectively. A. KO female mice were sham-operated or ovariectomized at 7 to 8 weeks of age. At ~3 months, the control group of sham-operated mice received vehicle (Veh), while ovariectomized mice received a single dose of E2 by intraperitoneal injection (50 µg/kg). n=6-7 mice. Like KO male mice, Ovx KO mice exhibit 2-fold lower sLDLR levels than sham-operated KO mice (t=0). They also respond to E2 by a peak of shedding culminating 20 hours post-injection. **B**. Two weeks later, the same mice than above (~3.5 months) received a single injection of ZLDI-8 (10 mg/kg). ZLDI-8 produced a drop in plasma sLDLR levels 8 hours post-injection in sham-operated mice only. *P* values were determined using 2-Way ANOVA followed by Tukey's multiple comparisons test.

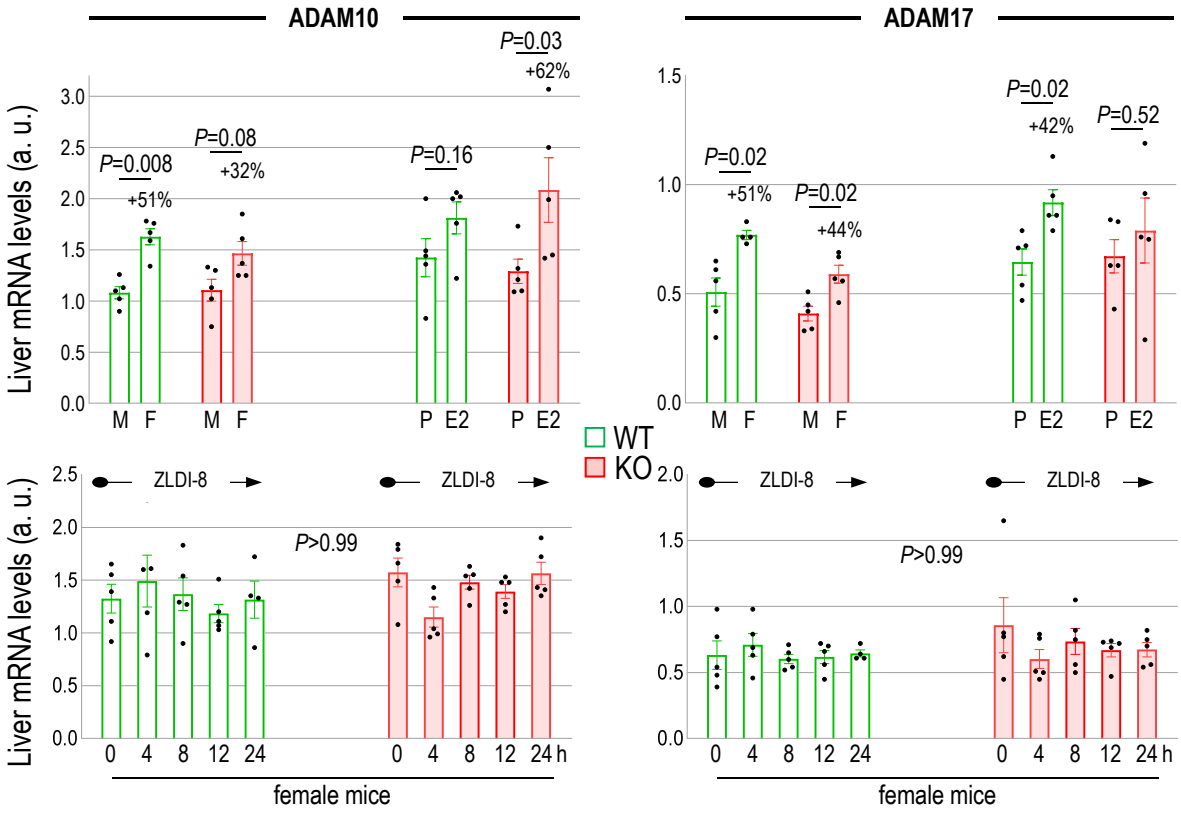

Figure S8. Neither PCSK9 deficiency nor ZLDI-8 affect ADAM10 and ADAM17 mRNA expression.
Liver mRNA levels of ADAM10 and ADAM17 were assessed by QPCR in the liver of all mouse models. They are sensitive to sex and/or E2 treatment, but unaffected by genotype or ZLDI-8 treatment. M, male; F, female; P, OvxP; E2, OvxE2. n= 5 mice. Mean±SEM. Difference between M/F or OvxP/E2 (upper panels) was determined using Mann-Whitney *U* test (non parametric data) and during ZLDI-8 treatment (lower panels) using Kruskal-Wallis test followed by Dunn's multiple comparisons test (non parametric data).

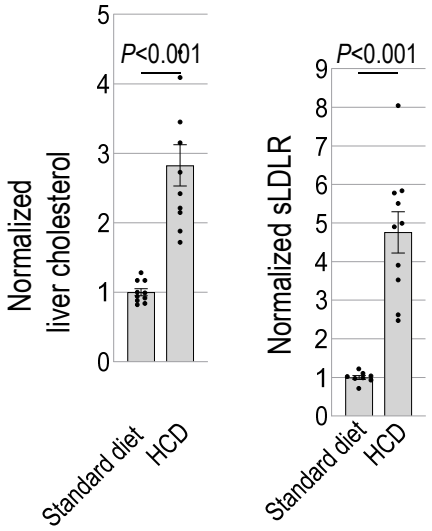

Figure S9. High cholesterol feeding increases LDLR shedding in KO male mice.
KO male mice were fed a standard laboratory diet supplemented with 0.45% cholesterol (ENVIGO; TD.08464) for 2 weeks, and liver cholesterol and sLDLR levels were measured. HCD, high cholesterol diet. n=10 mice. Mean±SEM. *P* values were determined using unpaired Student's t-test.

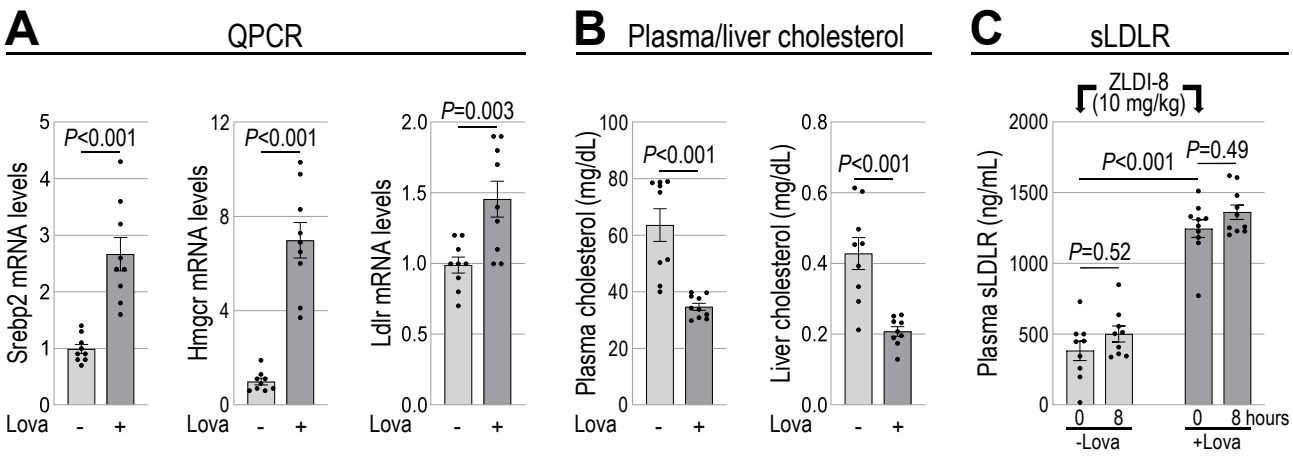

Figure S10. Lovastatin generates higher levels of sLDLR that are not sensitive to ZLDI-8. PCSK9 KO male mice were fed a regular laboratory diet containing or not 0.2% lovastatin for 10 days. Effect of lovastatin on: **A**, SREBP-2, HMG-CoA reductase and LDLR mRNA levels; **B**, plasma and liver cholesterol levels. **C**, sLDLR levels before of after ZLDI-8 injection. Note that the higher sLDLR levels observed upon lovasatatin treatment remained non-inhibitable by ZLDI-8. n=9-10 mice. Mean±SEM. *P* values were determined using unpaired Student's t-test (**A** and second panel in **B**), Mann Whitney *U* test (non parametric data; first panel in **B**), and 1-way ANOVA followed by Tukey's multiple comparisons test (**C**).

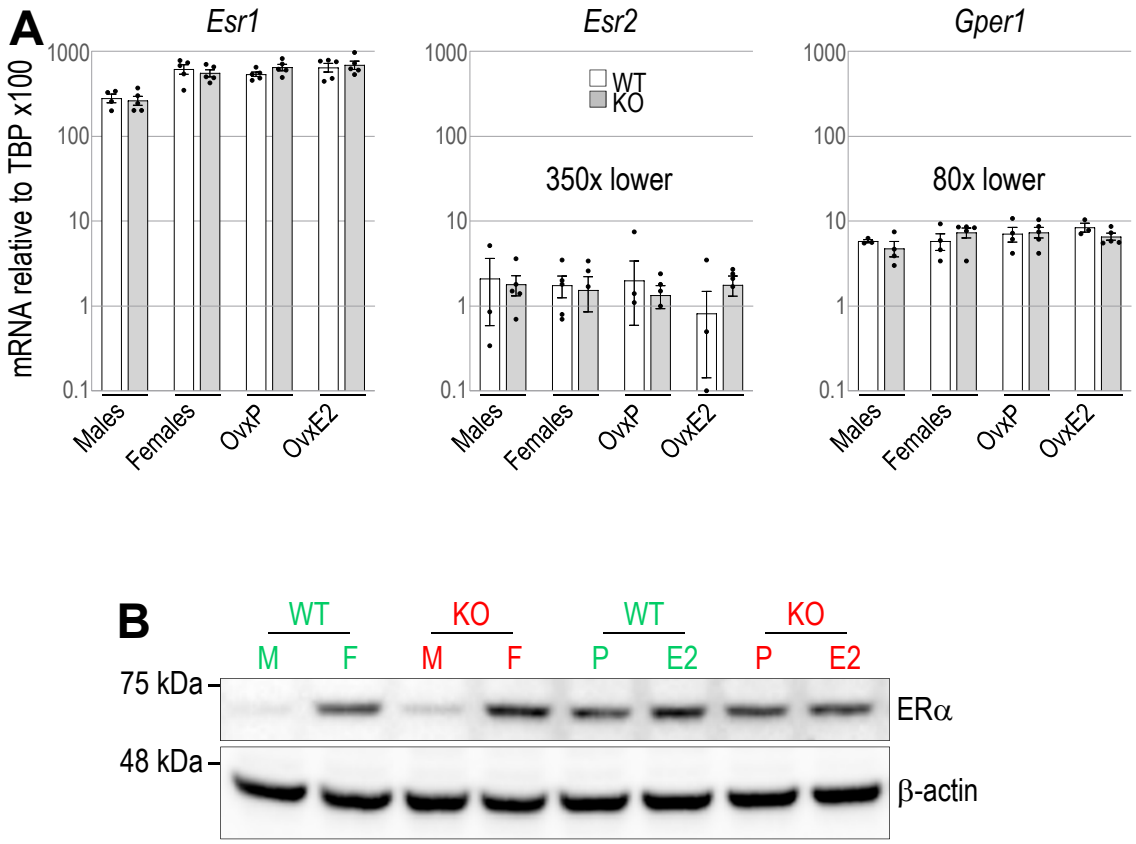

Figure S11. Liver expression of E2 receptors.
A, WT and KO livers were analyzed for their ERα (*Esr1*), ERβ (*Esr2*) or GPER (*Gper1*) mRNA content normalized to that of *Tbp*. n=5 mice. **B**, ERα and β-actin (apparent molecular weights were ~66 kDa and 42 kDa, respectively) were visualized in 30 ug of protein extracts (pools of 5 mouse extracts). Note that WT and KO female livers exhibit similar levels of ERα.

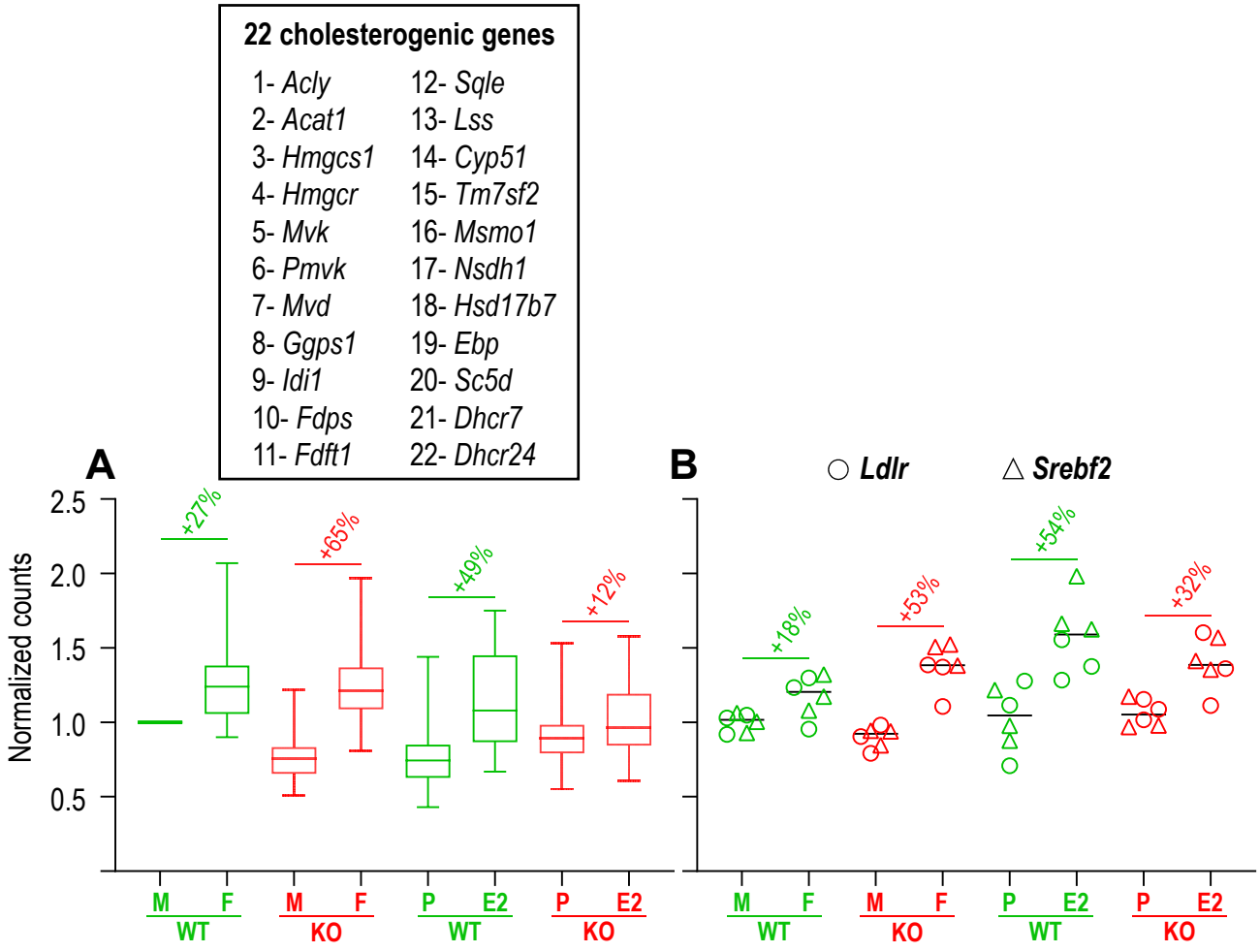

Figure S12. Regulation in our mouse models of cholesterogenic genes, including *Ldlr and Srebf2*.
RNA-Seq normalized counts were normalized to the average expression value in WT male livers set to 1. **A,** The box plot shows the expression of 22 cholesterogenic genes in WT (green) and KO (red) males (M), females (F), OvxP or OvxE2 livers. **B,** The dot plot illustrates the individual normalized expression of *Ldlr* (○) and *Srebf2* (Δ). n=3. The combined absence of PCSK9 and estrogen (KO male and OvxP) leads to the lowest cholesterol contents (*see* Figure 5) without SREBP2 pathway upregulation.

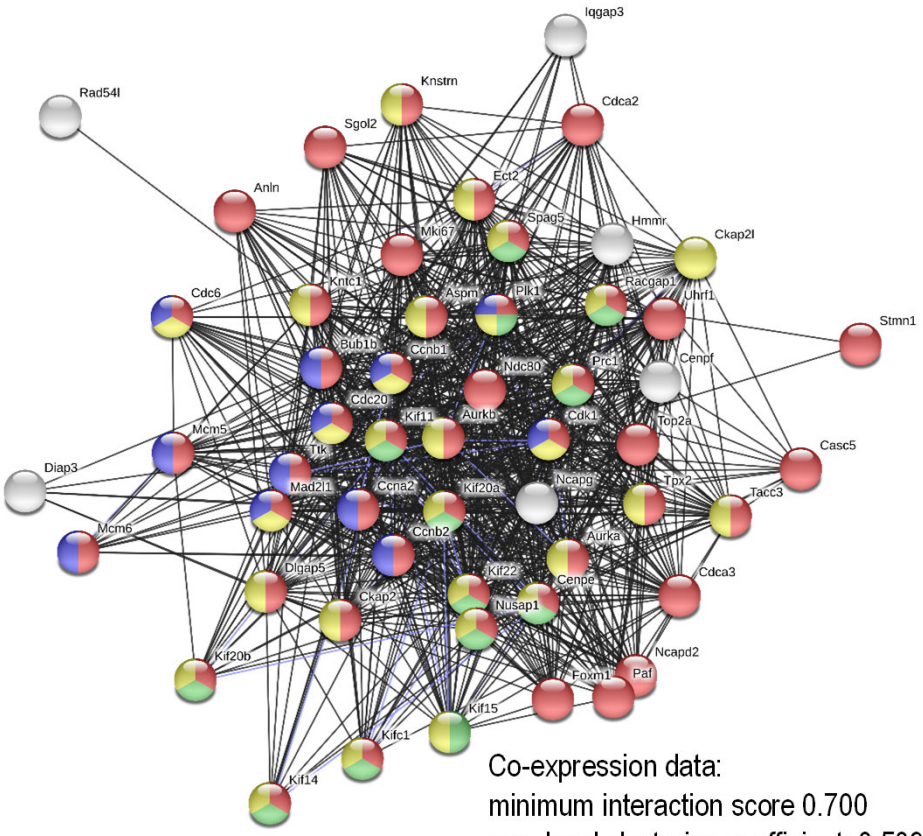

Co-expression data:
minimum interaction score 0.700
avg. local clustering coefficient: 0.589
protein-protein interaction enrichment *P*-value:< 10^{-16}

	term	FDR
KEGG pathway	cell cycle (mmu04110)	7.0E-14
Biological Process	cell cycle (GO:0007049)	7.7E-37
Molecular Function	microtubule binding (GO:0008017)	2.0E-09
Cellular Component	spindle (GO:0005819)	1.2E-29

Figure S13. Identification of a 54-gene cluster.
Using STRING [1] a cluster of 54 genes was identified. The average expression of these genes is increased by 116% in the absence of PCSK9, and strongly downregulated by E2 (-66%). Among them, 49 genes are related to the cell cycle, especially to the G2/M transition. Briefly, the later is controlled by cyclins B1 and B2 (*Ccnb1*, *Ccnb2*) that associate with CDK1 (*Cdk1*). The *Cenpe*, *Cenpf*, *Knl1* and *Ndc870* genes control the connection of chromosomal centromeres with spindle microtubules via kinetochores before segregation. *Aurkb*, *Ect2*, *Plk1*, *Prc1* and *Racgap1* genes are implicated in the preparation of the cleavage furrow, while *Bub1b*, *Cdc20*, *Mad2l1* and *Ttk* control the activity of the Anaphase Promoting Complex/Cytosome complex.

References

[1] D. Szklarczyk, A. Franceschini, S. Wyder, K. Forslund, D. Heller, J. Huerta-Cepas, M. Simonovic, A. Roth, A. Santos, K.P. Tsafou, M. Kuhn, P. Bork, L.J. Jensen, C. von Mering, STRING v10: protein-protein interaction networks, integrated over the tree of life, Nucleic Acids Res, 43 (2015) D447-452.

Roubtsova et al. (2022)

	term description	observed gene count	background gene count	FDR
Kegg				
mmu04110	Cell cycle	13	122	7.01E-14
mmu04914	Progesterone-mediated oocyte maturation	9	90	1.55E-09
mmu04114	Oocyte meiosis	8	112	1.44E-07
mmu04218	Cellular senescence	5	171	0.0039
mmu04115	p53 signaling pathway	3	66	0.0141
mmu05203	Viral carcinogenesis	4	199	0.0369
mmu03030	DNA replication	2	35	0.0396
Biological Process (GO)				
GO:0007049	cell cycle	47	1085	7.69E-37
GO:0051301	cell division	37	471	1.57E-36
GO:0000278	mitotic cell cycle	32	457	1.27E-29
GO:1903047	mitotic cell cycle process	31	404	1.27E-29
GO:0022402	cell cycle process	36	703	1.66E-29
GO:0000280	nuclear division	23	264	1.42E-22
GO:0010564	regulation of cell cycle process	28	554	5.20E-22
GO:0007059	chromosome segregation	22	251	1.06E-21
GO:0051726	regulation of cell cycle	33	954	1.06E-21
GO:0000819	sister chromatid segregation	18	120	2.24E-21
GO:0098813	nuclear chromosome segregation	20	193	4.95E-21
GO:0140014	mitotic nuclear division	18	131	7.99E-21
GO:0000070	mitotic sister chromatid segregation	15	94	4.84E-18
GO:0051983	regulation of chromosome segregation	15	97	6.92E-18
GO:0007017	microtubule-based process	25	595	7.58E-18
GO:0007051	spindle organization	15	119	1.00E-16
GO:0000226	microtubule cytoskeleton organization	21	401	1.39E-16
GO:1902850	microtubule cytoskeleton organization involved in mitosis	13	90	4.18E-15
GO:0051783	regulation of nuclear division	15	184	3.52E-14
GO:0051276	chromosome organization	25	883	4.61E-14
Molecular Function				
GO:0008017	microtubule binding	13	245	1.97E-09
GO:0015631	tubulin binding	14	336	3.20E-09
GO:0019900	kinase binding	17	737	9.83E-08
GO:0003777	microtubule motor activity	8	89	1.31E-07
GO:0005524	ATP binding	21	1389	6.48E-07
GO:0019901	protein kinase binding	15	659	6.48E-07
GO:0008092	cytoskeletal protein binding	16	877	2.38E-06
GO:0036094	small molecule binding	25	2364	1.02E-05
GO:0016887	ATPase activity	10	372	1.65E-05
GO:0000166	nucleotide binding	22	2006	2.43E-05
GO:0035173	histone kinase activity	4	22	2.56E-05
GO:0097367	carbohydrate derivative binding	22	2051	2.99E-05
GO:1990939	ATP-dependent microtubule motor activity	4	26	4.22E-05
GO:0005515	protein binding	43	6454	4.24E-05
GO:0017111	nucleoside-triphosphatase activity	12	714	0.00011
GO:0008574	ATP-dependent microtubule motor activity, plus-end-directed	3	13	0.0002
GO:0019899	enzyme binding	21	2175	0.0002
GO:0043168	anion binding	23	2578	0.00024
GO:0004672	protein kinase activity	10	593	0.00046
GO:0010997	anaphase-promoting complex binding	2	5	0.0019
Cellular Component				
GO:0005819	spindle	29	321	1.15E-29
GO:0000922	spindle pole	20	152	6.10E-23
GO:0015630	microtubule cytoskeleton	35	1106	2.62E-22
GO:0072686	mitotic spindle	17	89	4.71E-22
GO:0044430	cytoskeletal part	38	1460	6.89E-22
GO:0005874	microtubule	21	377	1.80E-17
GO:0099513	polymeric cytoskeletal fiber	23	581	3.50E-16
GO:0000775	chromosome, centromeric region	16	186	4.85E-16
GO:0043232	intracellular non-membrane-bounded organelle	48	3809	4.85E-16
GO:0000779	condensed chromosome, centromeric region	14	115	5.70E-16
GO:0000793	condensed chromosome	16	216	3.58E-15
GO:0000776	kinetochore	13	129	6.89E-14
GO:0030496	midbody	13	165	9.73E-13
GO:0005813	centrosome	18	481	2.03E-12
GO:0000777	condensed chromosome kinetochore	11	103	3.79E-12
GO:0000780	condensed nuclear chromosome, centromeric region	8	26	3.85E-12
GO:0005815	microtubule organizing center	20	682	5.20E-12
GO:0051233	spindle midzone	8	31	1.18E-11
GO:0005694	chromosome	22	929	1.68E-11
GO:0005871	kinesin complex	8	50	3.21E-10

Figure S14. Gene ontology.

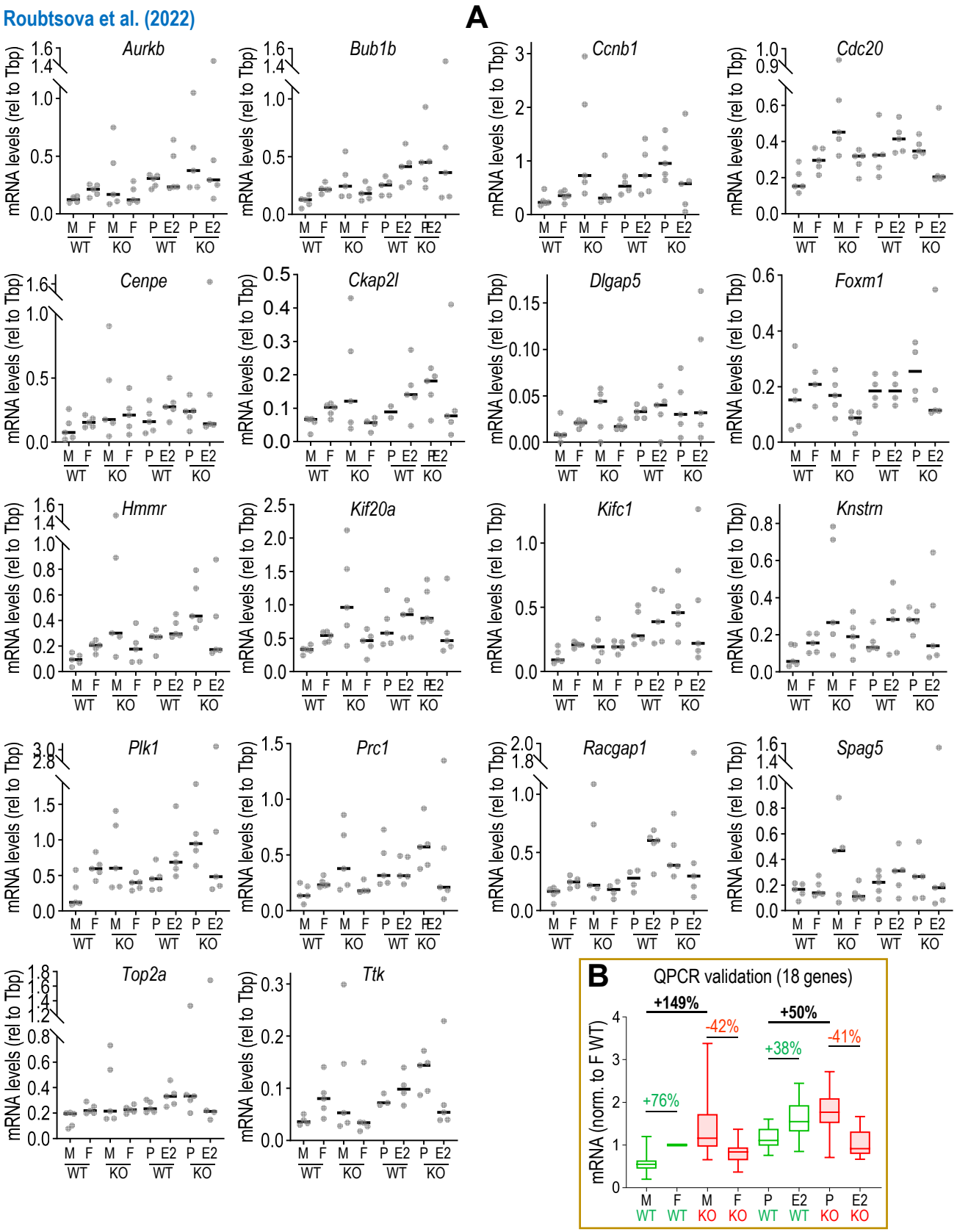

Figure S15. Genes in the STRING cluster have a pattern of expression associated with the surface LDLR phenotype.

A, The expression pattern of 18 genes belonging to the 54 gene-cluster was validated by QPCR. Median values are indicated. **B**, Box plot of the gene expression of the above 18 genes normalized to the average obtained for WT female mice and set to 1. Lower and upper boundaries of each box indicate the 25th and the 75th percentile, respectively. n=5 mice. Medians were compared (%).

Roubtsova et al. (2022)

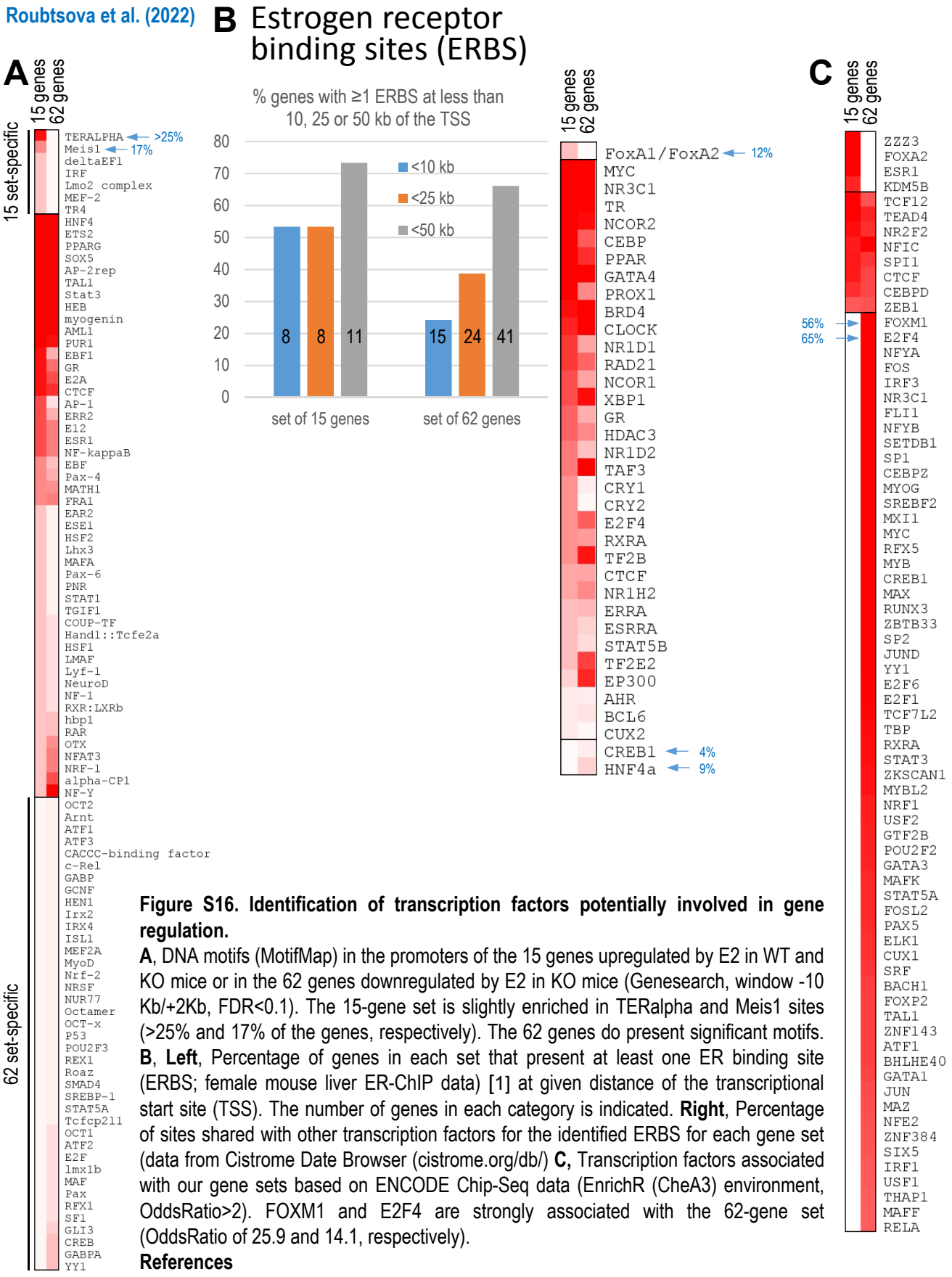

Figure S16. Identification of transcription factors potentially involved in gene regulation.

A, DNA motifs (MotifMap) in the promoters of the 15 genes upregulated by E2 in WT and KO mice or in the 62 genes downregulated by E2 in KO mice (Genesearch, window -10 Kb/+2Kb, FDR<0.1). The 15-gene set is slightly enriched in TERalpha and Meis1 sites (>25% and 17% of the genes, respectively). The 62 genes do present significant motifs. **B**, **Left**, Percentage of genes in each set that present at least one ER binding site (ERBS; female mouse liver ER-ChIP data) [1] at given distance of the transcriptional start site (TSS). The number of genes in each category is indicated. **Right**, Percentage of sites shared with other transcription factors for the identified ERBS for each gene set (data from Cistrome Date Browser (cistrome.org/db/) **C,** Transcription factors associated with our gene sets based on ENCODE Chip-Seq data (EnrichR (CheA3) environment, OddsRatio>2). FOXM1 and E2F4 are strongly associated with the 62-gene set (OddsRatio of 25.9 and 14.1, respectively).

References

[1] G. Palierne, A. Fabre, R. Solinhac, C. Le Péron, S. Avner, F. Lenfant, C. Fontaine, G. Salbert, G. Flouriot, J.F. Arnal, R. Métivier, Changes in Gene Expression and Estrogen Receptor Cistrome in Mouse Liver Upon Acute E2 Treatment, Mol Endocrinol, 30 (2016) 709-732.

Variables	Men	Pre-menopausal women	P value
Age (years)	42 (37-49)	42 (38-44)	1.00
LDL-C (mmol/L)	0.78 (0.60-1.63)	0.90 (0.63-1.42)	0.65
sLDL (ng/mL)	99 (29-118)	130 (110-171)	0.03

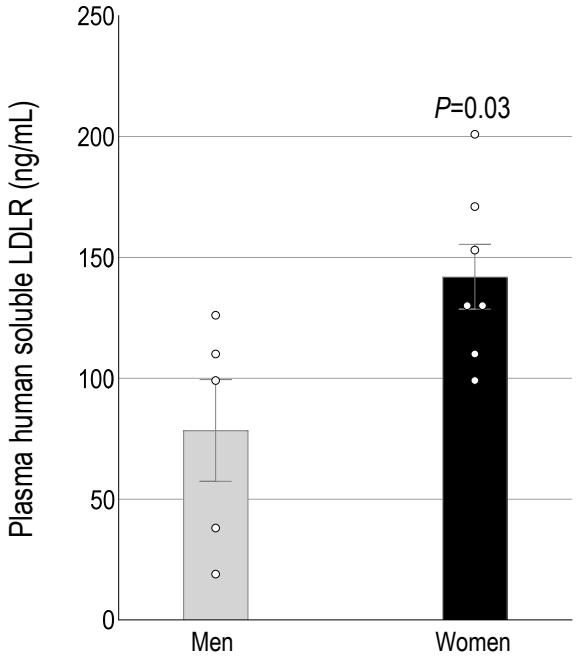

Figure S17. Plasma levels of human shed LDLR in PCSK9 mAb-treated men and premenopausal women. Plasma from men and pre-menopausal women was analyzed after ≥2 months of PCSK9 inhibitor treatment. Their age, plasma LDL-cholesterol and sLDLR content are indicated as median (Q1-Q3). The distribution of the sLDLR values is shown. n=5-7. Mean±SEM. *P* value was determined using Mann-Whitney U test (non-parametric).